Postprint of : Karami Horestani A., Shaterian Z., Mrozowski M., High Dynamic Range Microwave Displacement and Rotation Sensors Based on the Phase of Transmission in Groove Gap Waveguide Technology, IEEE SENSORS JOURNAL Vol 22 No 1 (2021), pp 182 - 189, DOI: 10.1109/JSEN.2021.3130658

High Dynamic Range Microwave Displacement and Rotation Sensors Based on the Phase of Transmission in Groove Gap Waveguide Technology

Ali K. Horestani, Zahra Shaterian, and Michal Mrozowski

***Abstract*— This research is focused on the design and realization of displacement sensors in gap waveguide technology. It is shown that with a small but fundamental change in the structure of a conventional gap waveguide, a linear displacement can be sensed. To this end, a unique feature of gap waveguides, i.e. the fact that no electrical connection between the top and bottom parts of the gap waveguide is required, is used. It is further shown that the concept can be also used for the development of rotation sensors. To validate the proposed concept linear and angular displacement sensors are designed and simulated. A prototype of the proposed linear displacement sensor is fabricated for demonstration. Agreement between the computed and measured results validates the concept.**

***Index Terms*— Displacement sensor, rotation sensor, gap waveguide technology.**

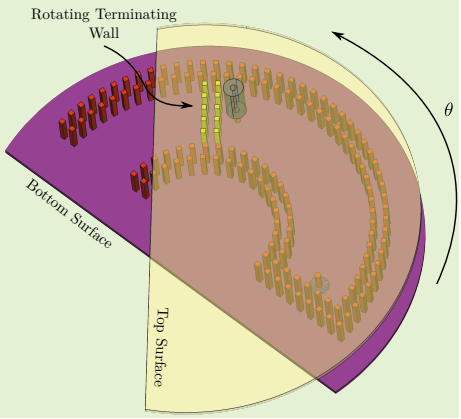

I. Introduction

Recent years have witnessed an increased interest in the application of RF and microwave technology for the development of various sensors such as humidity [1], [2], microfluidic [3], [4], material characterization [5], rotation [6]–[9], and displacement sensors [10]–[18]. These microwave sensors in terms of structure can be broadly classified in two categories: sensors based on the planar transmission line (TL) technology, and sensors based on waveguides or cavity resonators [2], [5], [19]. The sensors in the first category are low-cost, low-profile, and compatible with different technologies, and especially may be integrated with active microwave circuits. However, due to the presence of lossy dielectric materials, sensors in planar technologies generally suffer from relatively high loss especially at high frequencies, and as a result lower sensitivity and sensing accuracy. Moreover, scaling the sensors to higher frequencies would be desirable as it increases the sensitivity of displacement sensors. However, since the losses dramatically increase at higher frequencies, most planar microwave displacement and rotation sensors reported to date operate below 10 GHz. On the other hand, sensors based on metallic waveguides are usually bulky, however, they benefit from very low loss, therefore having very high-quality factor and sharp resonance, which are essential features for the realization of highly sensitive and accurate sensors. Furthermore, this category of sensors can be readily scaled to very high-frequency bands such as the millimeter-wave band to achieve significantly higher sensitivity.

It is important to note that while many types of sensors, including displacement and velocity sensors based on planar transmission lines are reported [6]–[14], [16]–[18], [20], [21], the application of waveguides and cavity resonators for the measurement of linear and angular displacement and velocity is very limited [16], [18], [19]. This is mainly because a conventional metallic hollow waveguide has an integrated structure, and even though the structure may be fabricated in separate sections, for the proper operation of the waveguide the sections have to be seamlessly connected with numerous screws. Therefore, the integration of a movable or rotatable part for the measurement of a linear or angular displacement is not an easy task.

To address this issue, in this research a relatively new waveguide technology, known as gap waveguide technology

This work was supported by Gdańsk University of Technology via research subsidy and NOBELIUM grant DEC-7/2020/IDUB/I.1 under the "Excellence Initiative – Research University" programme, and by Iran Technical and Vocational University via research grant 25/410/374.

All authors are with the Department of Microwave and Antenna Engineering, Faculty of Electronics, Telecommunications, and Informatics, Gdansk University of Technology, Narutowicza 11/12, 80-233 Gdansk, Poland.

A. K. Horestani is also with the Wireless Telecommunication Group, A&S Institute, Ministry of Science, Research and Technology, Tehran 64891, Iran, Email: alikaramih@gmail.com

Z. Shaterian is also with the Department of Electrical Engineering, Technical and Vocational University (TVU), Tehran, Iran.

is used [22], [23]. This technology was basically developed to overcome the problem of power loss due to an imperfect electrical connection between the sections of conventional hollow waveguides. With this aim, the gap waveguide technology takes advantage of the propagation bandgap provided by a parallel pair of a perfect electric conductor (PEC) and a perfect magnetic conductor (PMC) [24], [25]. In other words, it was shown that the sidewalls of a conventional waveguide can be readily replaced with the parallel PEC-PMC structure, provided the gap between the two surfaces is smaller than a quarter wavelength. Therefore, the waveguide bypasses the need for an electrical connection between the bottom and top conductive surfaces.

So far, this feature of gap waveguides has been mainly used to overcome the power loss issue due to imperfect electrical connections between the sections of conventional waveguides. However, another important consequence of the possibility of having two separate sections in gap waveguides, which is the main principle behind the sensors presented in this paper, is that the top and bottom sections of a gap waveguide can have relative movements. In short, the focus of this study is to show that a relative displacement or rotation of the top and bottom conductive surfaces of a gap waveguide resonator can be used for the measurement of linear and angular displacements in the millimeter frequency range. The main concept and required modifications in the structure of a gap waveguide cavity resonator for sensing linear displacement as well as the numerical results are presented in the next section. Section III is devoted to the validation of the concept and numerical results through the fabrication and measurement of a prototype of the proposed displacement sensor. It is further shown in Section III that the same concept can be used for the development of a rotation sensor. A discussion on the pros and cons of the proposed sensors in comparison to the displacement sensors based on other methods is presented in Section V. Finally, the paper is concluded in Section VI.

II. Linear Displacement Sensor in Gap Waveguide Technology

Fig. 1(a) shows an illustration of the conventional implementation of a groove gap waveguide cavity resonator [26]. The structure is composed of the bottom and top conductive surfaces that are separated by an air gap. The bottom conductive surface is equipped with arrays of conductive pins. These conductive pins that are about a quarter wavelength high at the desired operating frequency are short-circuited by the metallic surface on which they are implemented. Thus, they effectively produce a PMC surface at their open ends. Provided the distance between the open end of the pins and the top conductive surface is less than a quarter wavelength, the structure provides a cut-off condition for the propagation of EM waves. Therefore, the array of pins acts as the sidewalls that along with the top and bottom conductive surfaces form a gap waveguide cavity resonator.

As mentioned earlier in the introduction, one of the main limitations of conventional hollow waveguides for sensing displacement or velocity is that their structure is integrated. This

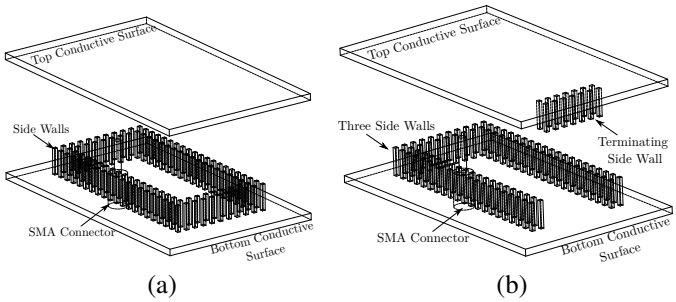

Fig. 1. Illustrations of (a) the conventional implementation of a groove gap waveguide cavity resonator, and (b) the proposed method for the implementation of a groove gap waveguide cavity for displacement sensing applications.

is in contrast to the gap waveguide technology in which no electrical connection between the bottom and top conductive parts is required, thus the two sections of the waveguide can have relative movements. However, note that if the top conductive surface of the cavity resonator of Fig. 1(a) is wide enough, as long as the distance between the bottom and top surfaces is unchanged, a horizontal displacement of the top surface with respect to the bottom surface does not have any effect on the resonance frequency or any other characteristic of the cavity. Therefore, the structure, in its current shape, cannot be used for sensing a displacement.

To address this issue, the structure of the cavity resonator is modified in this work. Fig. 1(b), shows the three-dimensional of the proposed method for the implementation of a gap waveguide cavity resonator with tunable resonance frequency. The structure is identical to the conventional gap waveguide cavity of Fig. 1(a) except that in the proposed cavity resonator three sidewalls are realized on the bottom conductive surface, while the terminating wall is realized by the array of metallic pins on the upper conductive surface. Note that, despite being implemented on different conductive surfaces, the walls provide the condition of non-propagation (cut off) of waves between the upper and lower metallic surfaces in any direction except inside the chamber. Therefore, the proposed structure very well works as a cavity resonator. However, in this configuration, with a longitudinal displacement of the top surface with respect to the bottom surface, the length of the cavity resonator and consequently its resonance frequency is changed. Therefore, the frequency of an oscillator which is built based on the proposed cavity resonator can be used for sensing a longitudinal displacement. Alternatively, the phase of the reflected or transmitted wave can be used for sensing a longitudinal displacement.

In the following, a displacement sensor based on the phase of transmission coefficient is presented. Figure 2 shows the top and side views of the proposed displacement sensor. The structure is similar to the cavity resonator of Fig. 1(b) with the following changes. 1) To have a two-port waveguide, a second coaxial port is introduced to the upper conductive surface, whereas the first port is mounted on the bottom surface. In this configuration, a relative longitudinal displacement of the two surfaces results in a change in the length of the waveguide as well as the distance between the two ports. As a result, the

phase of S_{21} depends on the displacement, and can be used for determining the amount of the displacement. 2) As shown in the figure, the side walls along the longitudinal direction of the cavity are long enough to maintain the integrity of the cavity such that the cavity resonator remains closed in all directions when the upper conductive surface along with the terminating wall of the cavity is moved in x direction. It is clear that the length of the extended sidewalls depends on the dynamic range of the sensor. Thus, the maximum measurable distance by the sensor is determined by the maximum possible length of the waveguide, which theoretically is infinite. Note that the minimum length of the cavity is determined by the minimum possible distance between the two ports. This length and its corresponding phase of transmission can be considered as the reference for the measurement of a displacement. However, note that before performing a displacement measurement an arbitrary position can be chosen as the zero position by recording its corresponding transmission phase as the reference phase. Then, a displacement with respect to the zero position can be sensed by measuring the actual phase of the transmission coefficient and calculating its difference with respect to the reference phase. With this explanation, it is clear that the minimum measurable distance is zero, and the sensor can sense both positive and negative displacements with respect to a zero position.

To validate the proposed method the structure of the displacement sensor of Fig. 2 is simulated using a full-wave EM simulator. The considered waveguide width is $w = 15.8$ mm, which corresponds to the width of a standard WR62 rectangular hollow waveguide for operation in the Ku band (12 to 18 GHz). The dimensions of the array of the pins are determined following the guidelines presented in [27]–[30] as: pin length $d = 6.25$ mm, pin width $a = 1$ mm, pins period $p = 2.7$ mm, and the air gap between the pins open end to the top conductive surface is $h = 1$ mm. The length and the position of each coaxial probe with respect to its corresponding terminating wall, as shown in the Fig. 2, are $g = 4.1$ mm and $s = 3.5$ mm, respectively.

The simulated phase of the transmission coefficient (versus frequency) for some values of displacements from 0 to 38 mm are depicted in Fig. 3. The results clearly show that an increase in Δx increases the absolute phase of the transmitted wave. Thus, the phase of S_{21} can be used for sensing the amount of displacement. The EM simulated (red dashed lines) absolute values of the phase of the transmission coefficient versus displacement Δx at the fixed frequencies $f = 13$ GHz to 17 GHz in steps of 1 GHz is plotted in Fig. 4. A linear relationship between the phase $\Delta\phi$ and the displacement Δx is observed, which is a desirable feature for sensor applications. The figure also shows the calculated (blue dotted lines) values of the phase of the transmission coefficient versus displacement based on

$$|\Delta\phi| = \beta|\Delta x| = \sqrt{(\frac{2\pi f}{c})^2 - (\frac{\pi}{w_{eff}})^2} \times |\Delta x|, \qquad (1)$$

where w_{eff} is the effective width of the gap waveguide that can be achieved based on the eigen-mode analysis of the waveguide unit cell [30], f is the frequency of operation, and

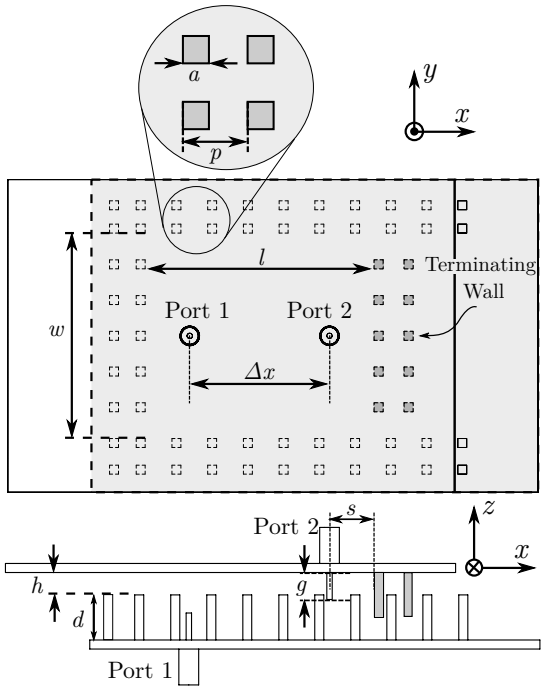

Fig. 2. Top and side views of the proposed groove gap waveguide structure for linear displacement sensing.

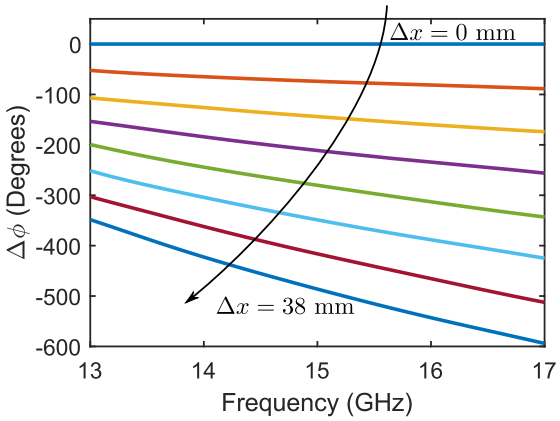

Fig. 3. The simulated phase of the transmission coefficient (versus frequency) for some values of displacements Δx from 0 to 38 mm.

Δx is the amount of displacement. Based on the very good agreement observed between the simulated and calculated values it can be inferred that the equation can be used to accurately determine the amount of a displacement Δx from its corresponding measured $\Delta\phi$. It is worth noting that since a one-to-one relation exists between the phase of the transmission coefficient and the amount of displacement, the sensor can also detect the direction and the velocity of a displacement. Another important point, as can be seen in the figure, is that the slope of the lines i.e. $d\phi/dx$, which shows the sensitivity of the sensor, increases at higher frequencies. Thus, scaling the sensor to higher frequency bands such as the millimeter-wave band to achieve higher sensitivities is another advantage of the proposed sensor, which is not feasible in planar technologies.

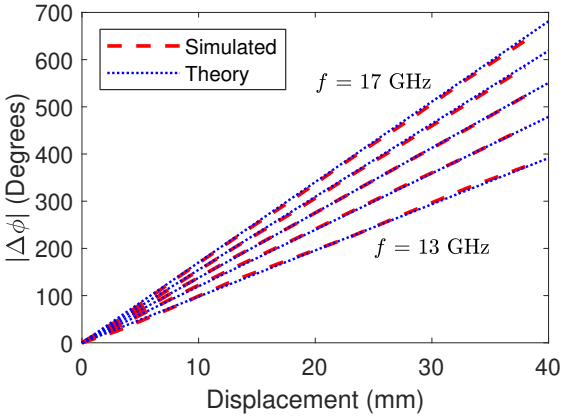

Fig. 4. EM simulated (red dashed lines) and theoretical (blue dotted lines) absolute values of the phase of S_{21} versus displacement Δx at the fixed frequencies f = 13 to 17 GHz in steps of 1 GHz.

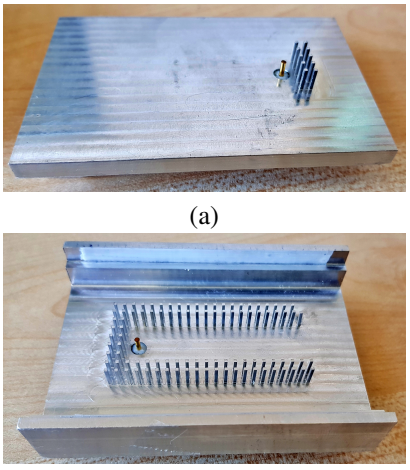

(a)

(b)

Fig. 5. Photographs of the fabricated linear displacement sensor. (a) Upper section, and (b) bottom section of the prototype. The rims on top of which the upper conductive surface is mounted can be seen in the photograph of the bottom section.

III. Experimental Results

To validate the proposed concept and numerical results, a prototype of the linear displacement sensor of Section II is fabricated and measured. Photographs of the top and bottom sections of the fabricated prototype are depicted in Fig. 5. As shown in the photographs, in addition to the arrays of pins that form the three sidewalls of the waveguide, the bottom surface of the structure is also equipped with a pair of rims to maintain the fixed gap between the top and bottom surfaces. The rim is also corrugated to limit the displacement of the top conductive surface only to the longitudinal direction of the waveguide. All dimensions of the fabricated prototype correspond to the simulated structure.

The measured phase shifts $\Delta\phi$ of the prototype versus frequency for different values of relative displacements Δx from 0 mm to 38 mm are depicted in Fig. 6. The figure clearly shows that the relative displacement of the top surface with respect to the bottom surface leads to the variation of the phase of S_{21}. Therefore, the phase $\Delta\phi$ can be used to sense a displacement Δx. Plots of EM simulated and measured phase

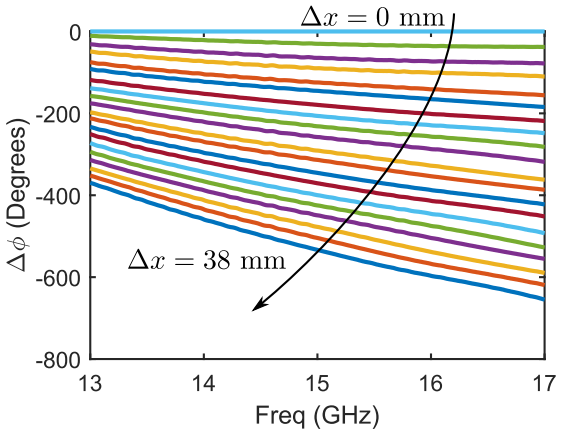

Fig. 6. The measured transmission phase shifts $\Delta\phi$ versus frequency for the fabricated prototype for different values of relative displacements Δx from 0 mm to 38 mm in steps of 2 mm.

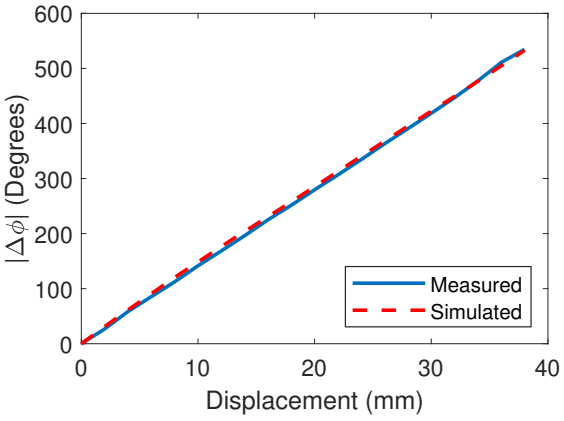

Fig. 7. A comparison between the absolute values of the simulated and measured phase shifts $\Delta\phi$ versus displacement Δx at f = 15 GHz.

shifts $\Delta\phi$ versus displacement Δx are depicted in Fig. 7, in which a good agreement between the simulated and measured results is observed. The figure also shows that the numerically computed linearity of the sensor is also confirmed by the experimental results.

To investigate the causes behind the small difference between the simulated and measured results the following possible sources of error are considered: 1) Slight fabrication misalignment in the place of ports. To this end, EM simulation of the structure for different values of transversal misalignment of the ports is conducted. The simulated phase shifts $\Delta\phi$ versus frequency for different values of transversal displacement of one port from zero to 1 mm in steps of 0.2 mm are depicted in Fig. 8. The figure shows that the phase variation due to 1 mm misalignment is less than 3 degrees at 15 GHz. Note that 1 mm is a significant misalignment and is just used to demonstrate the robustness of the sensor to such tolerances. A more realistic fabrication tolerance of 0.1 mm leads to 0.3 degree error in the transmission phase. 2) Small displacement of the top conductive plate with respect to the bottom one in vertical and transverse directions. As mentioned earlier and is clear in the photographs of the fabricated prototype, in the presented sensor such issue is avoided by devising a

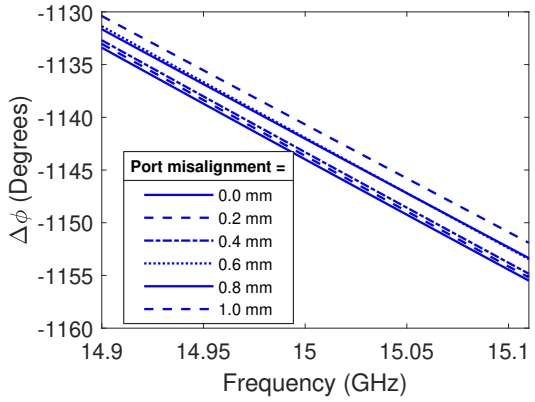

Fig. 8. Simulated phase shifts $\Delta\phi$ versus frequency for different values of transversal displacement of the ports from zero to 1 mm in steps of 0.2 mm.

corrugated rim on the bottom conductive plate on which the top plate is mounted. Therefore, the displacement of the top conductive surface is limited to the longitudinal direction of the waveguide. 3) Inaccuracies in the measurement process. Based on the discussion above it can be inferred that the small discrepancies between the numerical and experimental results are due to the limited accuracy of the measurement setup and fabrication tolerances.

IV. Development of an Angular Displacement Sensor in Gap Waveguide Technology

In the previous sections it was shown that with some modifications in the implementation of sidewalls, a gap waveguide can be used for the realization of a linear displacement sensor with high linearity and literary no limit in dynamic range. In this section, it is demonstrated that the same concept can be used for the design of rotation sensors. To this end, as shown in Fig. 9, the structure of the linear displacement sensor of the previous section is changed to a circularly curved gap waveguide. Again, the arrays of pins that form the two sidewalls and the initial wall of the waveguide as well as the feeding probe are implemented on one of the conductive surfaces (in this case on the lower conductive surface), whereas the pins of the terminating wall as well as the output probe are implemented on the other conductive surface (in this case the upper conductive surface). Therefore, an angular displacement of the upper conductive surface relative to the lower conductive surface leads to changes in the length of the waveguide. Consequently, changes in the phase of the transmission coefficient of the structure can be used to sense the amount of a rotation.

Note that, as illustrated in Fig. 9, the sidewalls of the cavity have to be long enough to maintain the integrity of the cavity when the upper conductive surface and the terminating wall rotates to the desired maximum measurable rotation angle. It is clear that the maximum measurable angle with the sensor of Fig. 9 is close to 180 degrees. This value can be increased up to 360 degrees by further extending the sidewalls of the waveguide. Also, the minimum measurable angle is the angle at which the output port reaches the input port, which is

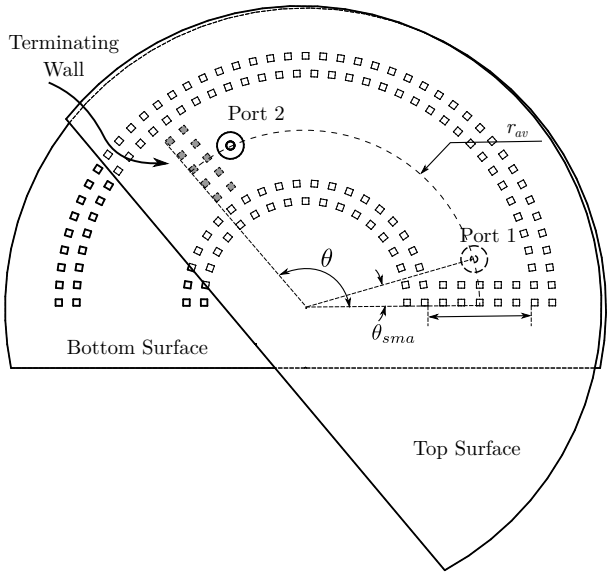

Fig. 9. Top view of the proposed angular displacement sensor. Port 2 and grayed pins are implemented on the top conductive surface, whereas port 1 and other pins are implemented on the bottom surface.

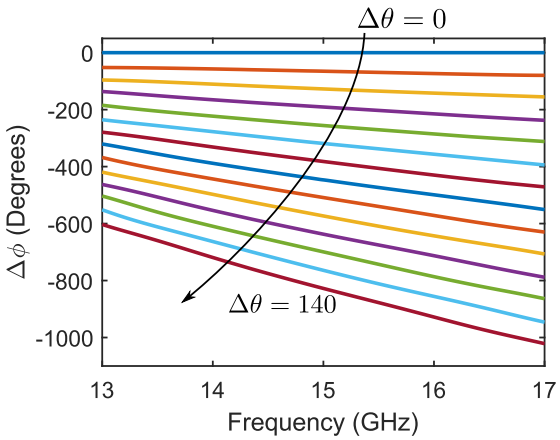

Fig. 10. Simulated phase of the transmission coefficient (versus frequency) for some values of rotation angle $\Delta\theta$ from 0 to 140 degrees.

40 degrees for the sensor of Fig. 9. Thus, considering the minimum angle as the reference, the dynamic range of the rotation sensor of Fig. 9 is about 140 degrees. The dynamic range can be readily increased to 320 degrees by extending the waveguide.

It is worth reminding that similar to the linear displacement sensor, the sensor also can be used as a single-port structure, in which changes in the phase of reflection coefficient or changes in the resonance frequency are used for sensing the amount of an angular displacement.

To validate the proposed method the structure of the rotation sensor of Fig. 9 is simulated using a full-wave EM simulator. The waveguide width is $w = 15.8$mm, and its average radius is $r_{av} = 27$ mm. Other dimensions of the structure are: pin length $d = 6.25$ mm, pin width $a = 1$ mm, and the air gap between the open end of the pins to the top conductive surface is $h = 1$ mm. The length and the distance between the coaxial probes and corresponding terminating walls are $g = 4.1$ mm and $s = 4.13$ mm, respectively. The period of pins in the

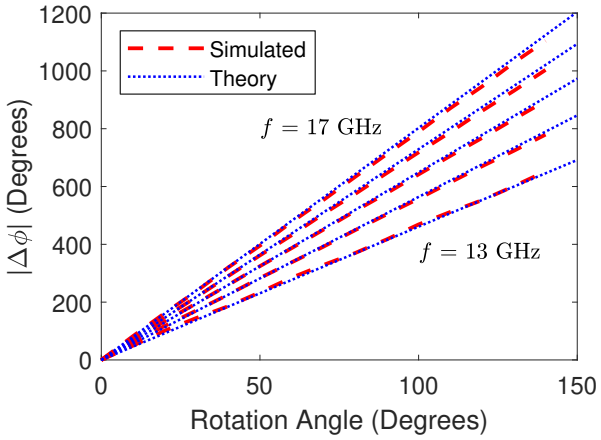

Fig. 11. EM simulated (red dashed lines) and theoretical (blue dotted lines) absolute values of the phase of S_{21} versus rotation angle $\Delta\theta$ at the fixed frequencies $f = 13$ to 17 GHz in steps of 1 GHz.

radial direction is $p = 2.7$ mm. However, to have an integer number of pins in the azimuth direction, the period of pins in that direction might be slightly different from $p = 2.7$ mm. Since the difference is not significant, it does not have a major effect on the behavior of the waveguide.

The simulated phase of the transmission coefficient (versus frequency) for some values of rotation angles are depicted in Fig. 10. Note that in this figure, the rotation angle $\theta_{sma} = 40°$ is considered as the reference. Therefore, rotation angle with respect to the reference angle is defined as $\Delta\theta = \theta - \theta_{sma}$, and $\Delta\phi = \angle S_{21}(\theta) - \angle S_{21}(\theta_{sma})$ is the phase of transmission coefficient at the angle θ with respect to the reference angle θ_{sma}. The results clearly show that an increase in the rotation angle θ increases the absolute value of $\Delta\phi$.

Graphs of the EM simulated (red dashed lines) absolute values of $\Delta\phi$ versus rotation angle $\Delta\theta$ at the fixed frequencies $f = 13$ GHz to 17 GHz in steps of 1 GHz is shown in Fig. 11. The figure shows a linear relation between $|\Delta\phi|$ and the angle of rotation $\Delta\theta$ that indicates that the phase of S_{21} can be used for sensing a rotation angle. The figure also shows the calculated (blue dotted lines) values of the phase of the transmission coefficient versus the angle of rotation based on

$$|\Delta\phi| = \beta|\Delta l| = \sqrt{(\frac{2\pi f}{c})^2 - (\frac{\pi}{w_{eff}})^2} \times |\Delta\theta| \times r_{av}, \quad (2)$$

where $|\Delta\theta|$ is the angle of rotation in units of radian and r_{av} represents the average radius of the waveguide. The good agreement between the simulated and calculated values again shows that the above equation can be used to accurately determine the rotation angle $\Delta\theta$ from its corresponding measured $\Delta\phi$. Also, it is observed that the slope of the lines, or in other words the sensitivity of the sensor, increases as the operating frequency of the sensors is increased. Higher sensitivities may be achieved by scaling the sensor down to a smaller size.

V. Pros and Cons of the Proposed Sensing Method

This section is devoted to a discussion on the advantages and limitations of the proposed linear and angular displacement sensing method based on the variations of transmission phase in comparison to other categories of microwave displacement sensors, namely, those based on a shift in resonance frequency and variation in depth of a notch (i.e., the amplitude of a signal). The comparison is conducted in terms of the most important parameters in sensing applications, namely, dynamic range, sensitivity, immunity to noise, operating frequency, and robustness to ambient conditions.

- *Dynamic range:* Generally, microwave sensors based on a depth of notch have a limited dynamic range, which is usually imposed by the limited sensitivity of the power meter circuits and reaching the noise level [6], [10], [13], [31]. In contrast, having a relatively higher dynamic range is one of the advantages of the displacement sensors based on the shift in the resonance frequency [12], [31], [32]. As demonstrated in the previous sections, the proposed linear displacement sensor has no limit in this regard, and can have a very wide dynamic range.
- *Sensitivity:* In most of the displacement sensors, higher sensitivity is achieved at the cost of a lower dynamic range [31], [33]. However, in the presented sensor, the dynamic range can be adjusted based on the application requirements by changing the waveguide length without any adverse effect on its sensitivity. This is because the sensitivity of the proposed sensor is a function of propagation constant, which depends only on the transverse dimensions of the waveguide and is independent of its length. Moreover, the sensor operates in mm-wave range, thus, gives relatively high sensitivity. The sensitivity can be further increased by scaling the sensor to operate at higher frequencies.
- *Immunity to noise:* Another unique feature of the proposed sensor is that unlike displacement sensors based on planar technologies that are prone to environmental noise and electromagnetic interference (EMI), the proposed sensor benefits from very good electromagnetic compatibility because the microwave signal is enclosed in the groove gap waveguide structure and is completely isolated from unwanted interfering signals. This unique feature might be useful in industrial applications where a high level of noise and EMI exist. Note that in addition to the provided isolation, since the phase and frequency of a signal are less prone to noise, sensors based on variation in phase or frequency are generally more immune to noise, compared to those based on changes in the amplitude of a signal.
- *Operating Frequency:* Another advantage of the proposed sensor is that it operates at a fixed frequency, thus can be used with a relatively simple and low-cost readout circuit. Note that despite having a variable operating frequency, the sensors based on a shift in the resonance frequency may have relatively simple and low-cost readout circuits. In contrast, variation of operating frequency for the sensors based on the depth of notch leads to relatively sophisticated and costly readout circuits [10].
- *Linearity:* Since the relation between a displacement and the resonance frequency of a resonator or the depth of

TABLE I

SUMMARY OF THE PROS AND CONS OF THE PROPOSED DISPLACEMENT SENSING METHOD IN COMPARISON TO DISPLACEMENT SENSORS BASED ON A SHIFT IN THE RESONANCE FREQUENCY OR CHANGES IN THE DEPTH OF NOTCH.

	Resonance Frequency	Depth of Notch	Phase (This work)
Dynamic Range	Moderate	Low	Very High
Sensitivity	Moderate	High	High
Immunity to Noise	High	Low	Very High
Operating Frequency	Variable	Fixed/Variable	Fixed
Linearity	Nonlinear	Nonlinear	Linear
Environmental Changes	Moderate	High	Moderate

resonance is not linear, most sensors based on these methods suffer from moderate to relatively high nonlinearity. In contrast, as shown theoretically by equation (1), the phase $\Delta\phi$ of transmission coefficient is a perfectly linear function of displacement Δx. This linear relation is also demonstrated in the previous sections by computational and experimental results.

- *Robustness to ambient conditions:* Most displacement sensors, especially those based on a shift in the resonance frequency, are quite sensitive to environmental changes such as changes in temperature. To minimize such adverse effects, sensors based on the symmetry properties of resonators have been developed. This method, which has been used for the realization of both sensors based on the variation of amplitude [6], [10] and sensors based on a shift in the resonance frequency [12], [14] is quite robust to environmental changes. However, since a similar method is not used in the presented displacement sensor, it is expected to be relatively sensitive to high temperature variations. However, knowing the thermal expansion coefficient of the waveguide material, the changes in the length of the waveguide due to temperature can be accurately calculated and considered to correct the measured displacement.

In short, while the proposed sensors are relatively bulky, it provides very high dynamic range, good sensitivity, immunity to noise, fixed operating frequency, and almost perfect linearity. A summary of the discussion above on the pros and cons of the three categories of displacement sensors are presented in Table I [33], [34].

VI. CONCLUSION

A method for the design and realization of a linear displacement sensor in groove gap waveguide technology has been presented. As opposed to the conventional method for the realization of gap waveguides, the proposed sensor has been realized by implementing the sidewalls of a groove gap waveguide on both the top and bottom conductive surfaces of the waveguide. It has been shown that the proposed sensor benefits from very good linearity, sensitivity, immunity to noise, and theoretically unlimited dynamic range. A prototype of the designed linear displacement sensor has been fabricated, and the presented concept and simulation results have been validated experimentally. The same concept has been used for the design of a rotation sensor. It has been shown that the phase of the transmission coefficient has a one-to-one relation with the linear and angular displacements. Therefore, the sensors are also able to measure the direction and the velocity of a linear or angular displacement. Advantages of the proposed sensors in terms of several important aspects including dynamic range, linearity, and immunity to noise are highlighted. It has been also demonstrated that high sensitivities can be achieved by scaling the proposed sensors to high frequencies, a feature that is not easily available in planar displacement and rotation sensors.

REFERENCES

[1] A. Benleulmi, N. Boubekeur, and D. Massicotte, "A highly sensitive substrate integrated waveguide interferometer applied to humidity sensing," *IEEE Microwave and Wireless Components Letters*, vol. 29, no. 1, pp. 68–70, Jan. 2019.

[2] H. E. Matbouly, N. Boubekeur, and F. Domingue, "Passive microwave substrate integrated cavity resonator for humidity sensing," *IEEE Transactions on Microwave Theory and Techniques*, vol. 63, no. 12, pp. 4150–4156, Dec. 2015.

[3] A. Ebrahimi, W. Withayachumnankul, S. Al-Sarawi, and D. Abbott, "High-sensitivity metamaterial-inspired sensor for microfluidic dielectric characterization," *IEEE Sensors Journal*, vol. 14, no. 5, pp. 1345–1351, May 2014.

[4] A. Ebrahimi, J. Scott, and K. Ghorbani, "Ultrahigh-sensitivity microwave sensor for microfluidic complex permittivity measurement," *IEEE Transactions on Microwave Theory and Techniques*, vol. 67, no. 10, pp. 4269–4277, Oct. 2019.

[5] A. K. Jha and M. J. Akhtar, "A generalized rectangular cavity approach for determination of complex permittivity of materials," *IEEE Transactions on Instrumentation and Measurement*, vol. 63, no. 11, pp. 2632–2641, Nov. 2014.

[6] A. K. Horestani, D. Abbott, and C. Fumeaux, "Rotation sensor based on horn-shaped split ring resonator," *IEEE Sensors Journal*, vol. 13, no. 8, pp. 3014–3015, Aug. 2013.

[7] A. Ebrahimi, W. Withayachumnankul, S. F. Al-Sarawi, and D. Abbott, "Metamaterial-inspired rotation sensor with wide dynamic range," *IEEE Sensors Journal*, vol. 14, no. 8, pp. 2609–2614, Aug. 2014.

[8] A. K. Jha, A. Lamecki, M. Mrozowski, and M. Bozzi, "A highly sensitive planar microwave sensor for detecting direction and angle of rotation," *IEEE Transactions on Microwave Theory and Techniques*, vol. 68, no. 4, pp. 1598–1609, Apr. 2020.

[9] A. K. Horestani, Z. Shaterian, and F. Martin, "Rotation sensor based on the cross-polarized excitation of split ring resonators (SRRs)," *IEEE Sensors Journal*, vol. 20, no. 17, pp. 9706–9714, Sep. 2020.

[10] A. K. Horestani, C. Fumeaux, S. F. Al-Sarawi, and D. Abbott, "Displacement sensor based on diamond-shaped tapered split ring resonator," *IEEE Sensors Journal*, vol. 13, no. 4, pp. 1153–1160, Apr. 2013.

[11] J. Naqui and F. Martin, "Transmission lines loaded with bisymmetric resonators and their application to angular displacement and velocity sensors," *IEEE Transactions on Microwave Theory and Techniques*, vol. 61, no. 12, pp. 4700–4713, Dec. 2013.

[12] A. K. Horestani, J. Naqui, Z. Shaterian, D. Abbott, C. Fumeaux, and F. Martín, "Two-dimensional alignment and displacement sensor based on movable broadside-coupled split ring resonators," *Sensors and Actuators A: Physical*, vol. 210, pp. 18–24, Apr. 2014.

[13] A. Horestani, J. Naqui, D. Abbott, C. Fumeaux, and F. Martín, "Two-dimensional displacement and alignment sensor based on reflection coefficients of open microstrip lines loaded with split ring resonators," *Electronics Letters*, vol. 50, no. 8, pp. 620–622, Apr. 2014.

[14] J. Naqui, J. Coromina, A. Karami-Horestani, C. Fumeaux, and F. Martín, "Angular displacement and velocity sensors based on coplanar waveguides (CPWs) loaded with S-shaped split ring resonators (S-SRR)," *Sensors*, vol. 15, no. 5, pp. 9628–9650, Apr. 2015.

[15] A. K. Horestani, N. Varmazyar, F. Sadeghikia, M. T. Noghani, Z. Shaterian, and F. Martín, "On the applications of S-shaped split ring resonators (s-srr) in sensors, filters, and antennas," in *International Conference on Electromagnetics in Advanced Applications (ICEAA)*. IEEE, Sep. 2019, pp. 0485–0488.

[16] A. Soltan, R. Sadeghzadeh, and S. Mohammad-Ali-Nezhad, "Angular displacement sensor based on corrugated substrate integrated waveguide (CSIW)," *IETE Journal of Research*, pp. 1–6, Aug. 2020.

[17] S. Fericean, A. Hiller-Brod, A. D. Dorneich, and M. Fritton, "Microwave displacement sensor for hydraulic devices," *IEEE Sensors Journal*, vol. 13, no. 12, pp. 4682–4689, Dec. 2013.

[18] A. Soltan, R. A. Sadeghzadeh, and S. Mohammad-Ali-Nezhad, "High sensitivity simple structured displacement sensor using corrugated substrate-integrated waveguide (CSIW)," *IET Microwaves, Antennas & Propagation*, vol. 14, no. 5, pp. 414–418, Feb. 2020.

[19] P. Sharma, L. Lao, and G. Falcone, "A microwave cavity resonator sensor for water-in-oil measurements," *Sensors and Actuators B: Chemical*, vol. 262, pp. 200–210, Jun. 2018.

[20] A. H. Karami, F. K. Horestani, M. Kolahdouz, and A. K. Horestani, "Rotation sensor based on magnetic microrods," *IEEE Sensors Journal*, vol. 18, no. 1, pp. 77–82, Jan. 2018.

[21] A. H. Karami, F. K. Horestani, M. Kolahdouz, A. K. Horestani, and F. Martín, "2d rotary sensor based on magnetic composite of microrods," *Journal of Materials Science: Materials in Electronics*, vol. 31, no. 1, pp. 167–174, Dec. 2019.

[22] P.-S. Kildal, E. Alfonso, A. Valero-Nogueira, and E. Rajo-Iglesias, "Local metamaterial-based waveguides in gaps between parallel metal plates," *IEEE Antennas and Wireless Propagation Letters*, vol. 8, pp. 84–87, 2009.

[23] P.-S. Kildal, "Waveguides and transmission lines in gaps between parallel conducting surfaces," Aug. 2014, US Patent 8,803,638.

[24] ——, "Artificially soft and hard surfaces in electromagnetics," *IEEE Transactions on Antennas and Propagation*, vol. 38, no. 10, pp. 1537–1544, 1990.

[25] ——, "Three metamaterial-based gap waveguides between parallel metal plates for mm/submm waves," in *2009 3rd European Conference on Antennas and Propagation*, 2009, pp. 28–32.

[26] E. Rajo-Iglesias and P.-S. Kildal, "Groove gap waveguide: A rectangular waveguide between contactless metal plates enabled by parallel-plate cut-off," in *Proceedings of the Fourth European Conference on Antennas and Propagation*, 2010, pp. 1–4.

[27] ——, "Numerical studies of bandwidth of parallel-plate cut-off realised by a bed of nails, corrugations and mushroom-type electromagnetic bandgap for use in gap waveguides," *IET Microwaves, Antennas & Propagation*, vol. 5, no. 3, p. 282, 2011.

[28] E. Pucci, A. U. Zaman, E. Rajo-Iglesias, P.-S. Kildal, and A. Kishk, "Study of Q-factors of ridge and groove gap waveguide resonators," *IET Microwaves, Antennas & Propagation*, vol. 7, no. 11, pp. 900–908, Aug. 2013.

[29] A. K. Horestani and M. Shahabadi, "Balanced filter with wideband common-mode suppression in groove gap waveguide technology," *IEEE Microwave and Wireless Components Letters*, vol. 28, no. 2, pp. 132–134, Feb. 2018.

[30] Z. Shaterian, A. K. Horestani, and J. Rashed-Mohassel, "Design of slot array antenna in groove gap waveguide technology," *IET Microwaves, Antennas & Propagation*, vol. 13, no. 8, pp. 1235–1239, Mar. 2019.

[31] A. K. Horestani, Z. Shaterian, and F. Martín, "Detection modalities of displacement sensors based on split ring resonators: Pros and cons," in *2019 International Conference on Electromagnetics in Advanced Applications (ICEAA)*. IEEE, 2019, pp. 0479–0484.

[32] Z. Shaterian, A. K. Horestani, and C. Fumeaux, "Metamaterial-inspired displacement sensor with high dynamic range," in *META 2013 Conference*, 2013, pp. 274–276.

[33] J. Naqui, J. Coromina, F. Martín, A. K. Horestani, and C. Fumeaux, "Comparative analysis of split ring resonators (SRR), electric-LC (ELC) resonators, and S-shaped split ring resonators (S-SRR): Potential application to rotation sensors," in *Proceedings of 2014 Mediterranean Microwave Symposium (MMS2014)*. IEEE, Dec. 2014, pp. 1–5.

[34] A. K. Horestani, Z. Shaterian, D. Abbott, and C. Fumeaux, "Application of metamaterial-inspired resonators in compact microwave displacement sensors," in *2014 1st Australian Microwave Symposium (AMS)*, 2014, pp. 19–20.